Integrated Electrophoresis Systems for Biochemical Analyses

D.J. Harrison, Z. Fan, K. Fluri, K. Seiler
Dept. of Chemistry, University of Alberta, Edmonton, AB, Canada T6G 2G2

Abstract

Microfluidic systems have been micromachined in glass chips for systems intended for chemical analysis or sensing. Using electroosmotic pumping, voltages control the direction of fluid flow without the need for valves. Mixing of reagent solutions, chemical reactions and separation of compounds in mixures can be achieved.

Introduction

Microflow systems can be prepared in glass substrates using silicon micromachining techniques. These systems can offer advantages in performance relative to stand-alone sensors, as has been demonstrated for ISFET-based analyzers [1,2]. We have etched systems composed of complex networks of intersecting capillaries, in which chemical reactions, sample injection and separation of individual components of a sample can be achieved [3,4]. The systems use electroosmotic effects for fluid pumping at velocities up to about 1 cm/s in 20 μm capillaries. Electroosmotic pumping also allows control of the direction of fluid flow at the intersection of capillaries, without a need for valves or other moving parts. Separations are achieved using electrophoretic effects, i.e. the differing mobilities of ions within an electric field result in different migration rates and this leads to separation. The separations are as efficient as in conventional capillary electrophoresis systems, and can be an order of magnitude faster, owing to the short distances involved. We have shown we can separate and detect mixtures of amino acids within 3 to 14 sec [4] and even more rapid separations have been reported by Effenhauser et al. [5] The potential applications of such systems include miniaturized analytical systems that could compete with bench-top instruments or chemical sensors in terms of performance, analysis time or durability [3-7].

To practically realize the use of electroosmotic pumping in a complex manifold of channels it is necessary to develop an understanding of the factors that control flow within such systems, particularly at the intersection of two channels containing different solutions. One of the best ways to achieve this is to visually image the flow process within the channels [4]. In addition, the quantitative study of flow rates and study of the ability to control the direction of solvent flow using applied fields is required. In this report we present both images and quantitative studies of diffusional and convective mixing of solutions at channel intersections.

The applications of micromachined devices could be quite varied if the chips can be made versatile. Performing chemical reactions on-chip is a key aspect of extending the versatility of these devices. To this end we have demonstrated that a variety of device layouts can be used for mixing reagents on-chip, the first step in inducing a chemical reaction, and reaction of amino acids with a fluorescent label is presented.

Results and Discussion

Electrical Characteristics.

A device referred to as COCE was prepared, consisting of three channels intersecting at a T-shaped junction, and this was used to study the application of potential to all three solvent reservoirs simultaneously. The device geometry and the labeling scheme we have used for the channel reservoirs, lengths and resistances are shown in Figure 1. As a first step the impedance characteristics of the network were determined. The dc electrical impedance of the intersecting capillaries was modelled as a network of resistors, as is shown in Figure 1b, and the validity of the model was examined.

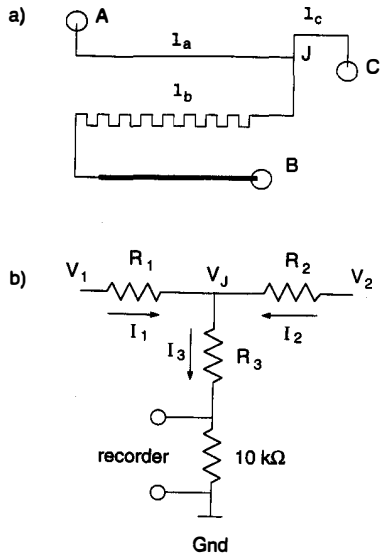

Figure 1. a) Device COCE layout with reservoir labels and channel lengths, l_x, indicated. Overall dimensions were 2.8 by 7.0 cm.
b) Equivalent circuit for device COCE. Subscripts refer generally to the resistances of the 3 channels of the device in a).

Table 1 gives the measured lengths and resistances between the reservoirs and the intersection point, and the ratios of these values to those for the channel length l_a. Channel length l_b consisted of both a 23 mm length that was 220 μm wide and a longer 30 μm wide segment. The wider segment length was expressed in terms of an equivalent length of 30 μm wide channel, specifically 3.1 mm, for the calculations. The data show that the resistances R_a, R_b, and R_c are indeed proportional to the channel lengths within experimental error, as would be expected providing there is no defect in the bonding of the glass cover plate to the etched piece.

Table I. Lengths and Resistances for COCE Device.

	A	B	C
Length (mm)	45	93.3	8
Resistance GΩ	0.32 ± 0.02	0.72 ± 0.02	0.079 ± 0.008
L/L_a	1	2.07 ± 0.03	0.18 ± 0.01
R/R_a	1	2.3 ± 0.2	0.25 ± 0.08

A,B,C refer to the lengths shown in Figure 1. Error in the lengths is about 0.5 mm. Ratios of lengths relative to L_a, and resistances relative to R_a are given.

0-9640024-0-X/hh1994/$20©1994TRF
DOI 10.31438/trf.hh1994.5

Solid-State Sensors, Actuators, and Microsystems Workshop
Hilton Head Island, South Carolina, June 12-16, 1994

With two voltage sources and a near ground potential connected to the channels, as illustrated in Figure 1b, the current in each channel and the potential at the intersection are readily expressed using Kirchhoff's Rules where the assumed directions of the currents I_1, I_2 and I_3 are shown in Figure 1b. The 10 kΩ resistor has been omitted, as it is much smaller than R_3. Solving for V_J and I_3 gives equations 1 and 2,

$$V_J = (V_1R_2R_3 + V_2R_1R_3) / (R_1R_2 + R_2R_3 + R_1R_3) \quad (1)$$

$$I_3 = [V_1R_2 + V_2R_1] / (R_1R_2 + R_2R_3 + R_1R_3) \quad (2)$$

While in general the potentials V_1 and V_2 can have any polarity, in this study V_1 was always positive and V_2 was always negative. Equation 2 shows that a plot of I_3 versus V_1 will be linear when V_2 is held constant, however I_3 may be positive or negative depending on the potentials applied and the resistance of each channel.

The behavior of the device with potentials applied to all three channels was evaluated according to the scheme indicated in the inset of Figure 2. The current was measured from the potential drop across a 10 kΩ resistor between ground and reservoir C, with V_1 and V_2 applied to reservoirs A and B, respectively. In this configuration the resistances for eq 1and 2 were $R_1 = R_a$, $R_2 = R_b$, and $R_3 = R_c$. The current was indeed linear in V_1 when V_2 was held constant. Figure 2 shows the data obtained for three different values of V_2. It was possible to calculate the current using eq 2 and the measured channel resistances given in Table 1, and the calculated response is shown as the solid lines in Figure 2. The very good agreement illustrated between theory and experiment shows that the model is accurate. It can be used to determine potentials and currents within a complex network of capillaries when several voltage sources are applied simultaneously.

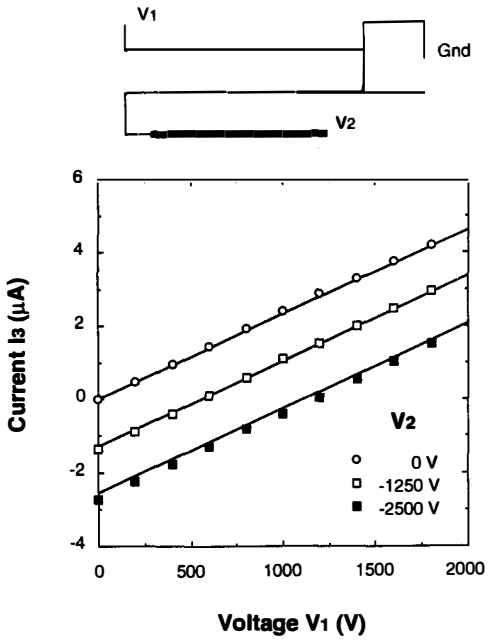

Figure 2. Current as a function of V_1 applied to reservoir A, with the indicated values of V_2 applied to reservoir B. Symbols are for experimental data, solid lines are for current calculated from equation 2 using the data in Table 1. The inset shows the applied potential scheme.

Leakage Control

We have previously discussed leakage effects at the intersection of channels [3-6]. In particular, if a side channel is left floating while a potential is applied to cause flow in the main channel there will be leakage of solution from the side channel, contaminating the main channel. We have indirectly shown that both convective and diffusion effects contribute to this mixing, or leakage effect at the intersection [3,4]. In previously studied devices with various layouts, the concentration of sample leaking into the main channel was about 3% of that in the sample channel. We show here that these effects can be controlled by applying voltages to several channels simultaneously.

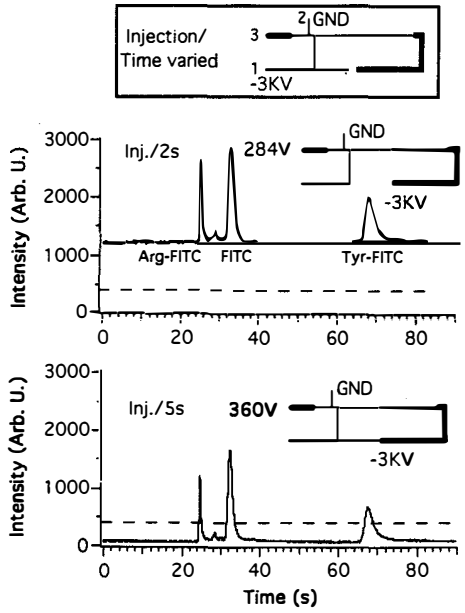

Figure 3. Separation of 20 μM Arg-FITC and 40 μM Tyr-FITC in 0.054 *M* carbonate buffer, pH 9.1, with potentials applied to three reservoirs of device Jet-1. The dashed line indicates the background level when the sample channel was instead left floating during separation.

Figure 3 shows data obtained in another device, Jet-1, with the layout indicated in the figure. The resistances of each of the channels of this device were determined as described above. The separation of fluorescein isothiocyanate (FITC) labelled arginine (arg) and tyrosine (tyr) is shown. For these experiments sample solution was present in reservoir 2, which was held at ground. As shown in the diagram at the top, samples were injected across a "double T" injector towards reservoir 1, which was at -3 kV. This injector creates a sample plug in the separation channel about 150 μm in length.

To evaluate the ability to control leakage during a separation we applied potentials to reservoirs 2, 3 and 4 simultaneously, as shown in the insets of Figure 3. In the first electropherogram of Figure 3, 284 V was applied to reservoir 3 during the separation. The background fluorescence level was high compared to the background seen when the sample channel was instead left floating (dashed line). From the

measured resistances of the channels the calculated potential at the intersection of the sample and separation channels should be -17 ± 12 V with 284 V on reservoir 3 and - 3 kV on reservoir 4. With the sample channel at ground there should be a net flow out of the sample channel resulting in an increased background, as was observed. When the potential at reservoir 3 increases, the potential at the injection point will eventually become positive, which should electroosmotically push sample solution back towards reservoir 2. As shown in Figure 3, 360 V at reservoir 3 lowered the background fluorescence below the level observed when the sample channel was left floating. The decrease in background showed that the flow in the sample channel was reversed, and establishes that leakage effects can be controlled using applied potentials.

Mixing of Solutions Using Voltage Control

When electroosmotic flow is present in a capillary the linear flow velocity, v, is given by eq 3,

$$v = (\mu_{eo} + \mu_{ep})E \quad (3)$$

where μ_{eo} and μ_{ep} are the electroosmotic and electrophoretic mobilities, respectively, and E is the electric field applied.[14]

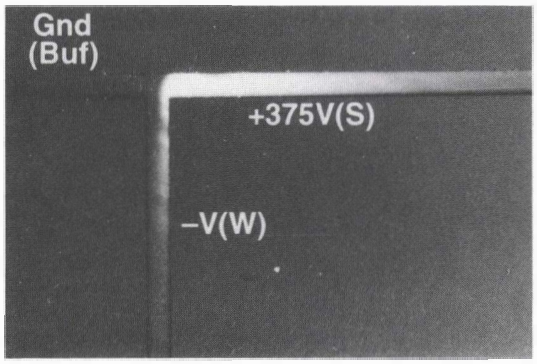

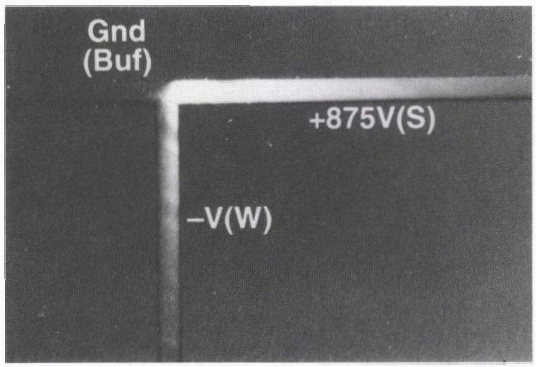

Figure 4. Photomicrographs showing controlled mixing of 10 mM carbonate buffer, pH 9.1, and 100 μM fluorescein. Channels are 30 μm wide. Flow direction was from the two horizontal channels into the vertical channel.

The overall mobility, μ, is the vector sum of these two mobilities, and μ_{eo} is generally larger than μ_{ep} in absolute terms. The velocity of species i in each of the channels is given by equations 4-6,

$$v_{i,1} = \mu_i (V_1 - V_J) / l_1 \quad (4)$$
$$v_{i,2} = \mu_i (V_2 - V_J) / l_2 \quad (5)$$
$$v_{i,3} = \mu_i V_J / l_3 \quad (6)$$

where V_J is given by eq 2, and the various v_i refer to the velocity of species i in each channel of length l. The subscripts 1, 2 and 3 refer to the velocity and channel length associated with the potential sources V_1, V_2 and ground, respectively. It is assumed the ionic strength (resistivity) and pH in each channel is the same. These expressions indicate that controlled mixing of solutions should be possible at the intersection of the three channels by adjustment of the potentials V_1 and V_2.

The COCE device was mounted under a microscope equipped with a camera and the region near the intersection was illuminated with 488 nm light. Any striations visible in the fluorescent dye stream seen in Figure 4 and later photos are due to non-uniformity in the illumination or collection efficiences, as is the tendency of the intensity to fade at the edges of the photos. Potentials were applied to the three reservoirs with the polarities indicated in Figure 4. Sample (S) was driven towards the waste reservoir (W), while buffer (Buf) was also driven towards waste by the applied potentials. The two solutions mixed downstream of the intersection. The data establish that increasing the potential on the sample reservoir increased the amount of dye relative to buffer downstream of the intersection.

Mixing chamber

Figure 5 shows the layout of a device called Jet-3, which has a mixing chamber incorporated. All channels of single line width are 30 μm wide, whereas the blackened bulky lines are 300 μm wide. The large box between in the figure was used as a mixing chamber. The chamber was 4.5 mm long and 170 μm wide. The volume of the chamber, excluding the islands, was about 3.6×10^{-3} mm^3. The offset between the side channels connected to reservoirs 3 and 4 was 220 μm .

Samples were introduced through reservoirs 1 and 2, while the other reservoirs and channels were filled with a buffer. To drive two different sample solutions through the chamber for mixing, a positive potential was applied to reservoir 1, with another applied to 2. Reservoir 3 was at ground. It is likely that diffusion served as the main driving force for mixing once the solutions were within the chamber, but this was not studied in detail. After a fixed time the potentials were switched off. Then the mixture in the chamber was injected through the double T injector. Application of a voltage between reservoirs 4 and 5 then caused the separation.

An example of mixing two solutions followed by their separation is shown in Figure 5. One solution contained fluorescein, while the other contained two labelled amino acids arginine and tyrosine. The bottom of the figure shows that all three components were observed when the sample plug was then separated. As a comparison, an electrophrogram without mixing is also shown in the top of Figure 5. In this case only the amino acid mixture was driven into the mixing chamber and the injector, so the final separation of the sample solution shows there is no fluorescein present.

On-column Reaction

Many chemicals are not detected using a fluorescence detection scheme unless they are chemically derivatized with

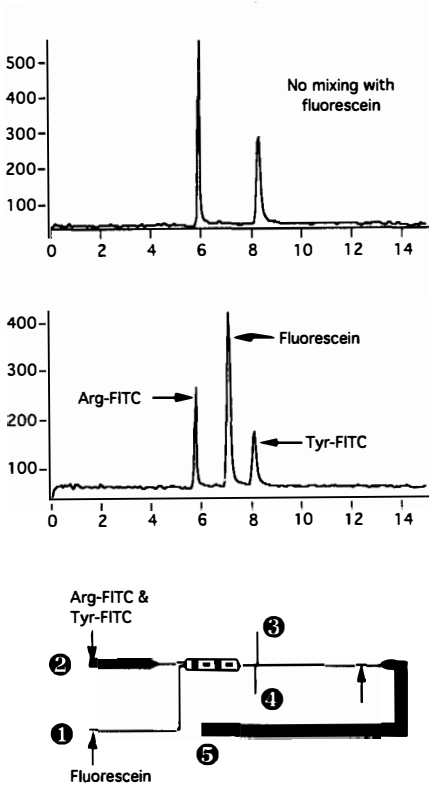

Figure 5. Layout of mixing chamber device. Top shows separation of amino acids, bottom shows separation of fluorescien from amino acids after mixing in chamber.

a fluorescent label. This reaction can be done before a separation is performed, but there are advantages if it is done after the separation. In chromatography this is known as post-column reaction, in electrophoresis it may be called a post-capillary reaction. This is a chemical reaction performed "on-the-fly" in the sample stream as it moves towards a detector, and it creates a fluorescent product when a sample is present. The most common reagent used for post-column derivatization is *o*-phthaldialdehyde (OPA), which reacts with primary amines to createa fluorescent product. It can be used to detect primary amines including amino acids.

We have performed some preliminary experiments with post-capillary reaction within a chip. The OPA reagent stream was delivered into the main separation channel from a side channel under potential control. The reaction was monitored a short distance downstream with a fluorescence detector, fluorescence being excited with a 325 nm laser. Pyrex glass has a fluorescent background at this excitation wavelength, so that the signal to noise performance is limited. Quartz or fused silica will be needed as the device substrate to improve this. Figure 6 shows the detection of an amino acid following reaction with OPA. The efficiency of the electrophoretic separation was degraded by the following OPA reaction, and some noise in the base line is apparent. It appears that these affects are due to the efficiency of mixing at the 90 ° intersection used in this device. Modifications in the mixer design have been made that are hoped will improve the efficiency and performance. Nevertheless, these results demonstrate that it is possible to perform chemical reactions within the chip that can be used to faciliate a chemical analysis.

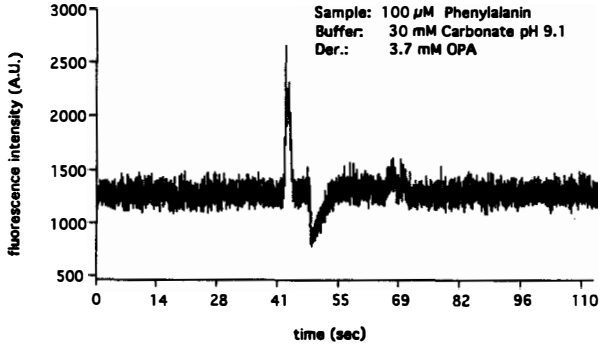

Figure 6. Post-capillary reaction of OPA with phenylalanine, evidenced by fluorescence detection.

Conclusions

This study has demonstrated the feasibility of using electroosmotic pumping to control flow in a manifold of flow channels without the use of valves. The fluidic control that can be achieved within these valveless devices allows for control of solution mixing, and enables us to effect reactions within the flowing streams. Biologically important molecules such as amino acids can be separated, allowed to react, and then detected, all within the confines of the chip, and within a few seconds. A number of different mixers can designed to perform these reactions, providing increased flexibility in terms of decreased problems from leakage at intersections and increased reaction times.

Acknowledgments

We thank Ciba-Geigy and NSERC of Canada for support. Z.F. thanks the Alberta Microelectronic Centre for a graduate fellowship and use of their facilities.

References

1. W. Olthus, B.H. van der Schoot, P. Bergveld *Sens. Actuat.* **17**, 279 (1989).
2. S. Shoji, M. Esashi, T. Matsuo *Sens. Actuat.* **14** , 101 (1988).
3. K. Seiler, D.J. Harrison, A. Manz *Anal. Chem. 65* (1993) 1481.
4. D.J. Harrison, K. Fluri, K. Seiler, Z. Fan, C.S. Effenhauser, A. Manz *Science 261* (1993) 895
5. Effenhauser, C. S.; Manz, A.; Widmer, H. M. *Anal. Chem.* **1993**, *65*, 2637-2642.
6. Harrison, D. J.; Manz, A.; Fan, Z.; Lüdi, H.; Widmer, H. M. *Anal. Chem.* **1992**, *64*, 1926-1932.
7. R.J. Gale, K. Ghowsi, in Biosensor Technology, Fundamentals and Applications, R.P.Buck, W.E. Hatfield, M. Umana, E.F. Bowder, Eds., Marcel Dekker, New York, **1990**, pp 55-62.